Mausam, (1990), **41**, 2, 234-240

551.509.33 : 551.21 : 535.651

Monsoon prediction at different resolutions with a global spectral model

T. N. KRISHNAMURTI

Florida State University, Tallahassee, Florida 32306, U.S.A.

सार – इस शोध पत्र के पहले भाग में मानसून क्षेत्र पर मध्य अवधि पूर्वानुमान प्रदर्शित किया गया है। FSU ग्लोबल स्पेक्ट्रल मॉडल में विभिन्न स्पेक्ट्रल वियोजनों T_{21}, T_{31}, T_{42} T_{63} और T_{106} का प्रयोग करते हुए उसी प्रारम्भिक डेटा बेस को आरम्भ करते हुए 5 दिनों के मानसून पूर्वानुमान के निष्पादन का परीक्षण किया गया है। उच्चतर वियोजन निदर्श (higher resolution models) अधिक यथार्थवादी वर्षण दर दिखाते हैं और आरम्भिक निवेश (initial input) से आरम्भ होती उपसारी पवन सामान्य मोड़ प्रारम्भीकरण प्रक्रिया अन्त में प्राप्त की गई है। उच्चतर वियोजनों का प्रयोग करते हुए निदर्श पूर्वानुमान इनकी गुणवत्ता में सम्पूर्णतः सुधार दिखाते हैं।

इस शोधपत्र का दूसरा भाग महीने के क्रम की अवधियों तक निम्न आवृति प्रणाली के पूर्वानुमान के लिए एक नया दृष्टिकोण प्रस्तुत करता है।

ABSTRACT. The first part of this paper illustrates medium range forecasts over the monsoon region. Using different spectral resolutions, T_{21}, T_{31}, T_{42}, T_{63} and T_{106} in the FSU global spectral model, the performance of the monsoon forecasts up to 5 days have been examined, starting with the same initial data base. The higher resolution models show more realistic precipitation rates and the divergent wind starting from the initial input that was obtained at the end of the normal mode initialization process. The model forecasts using higher resolutions show substantial improvement in their quality.

The second part of this paper addresses a new approach for the prediction of low frequency modes up to periods of the order of a month.

1. Medium range prediction at different horizontal resolution

The FSU global spectral model is a comprehensive physical model with detailed orography. It is currently being run with 12 vertical layers and 106 waves (Triangular truncation). The following are some of the details of this model :

The FSU Global Spectral Model

(A) *Outiline*

Domain — Global;

Dependent variables — Vorticity, divergence, temperature, dew point depression and the log of surface pressure (ζ, D, T, S, $\ln P_s$);

Vertical coordinate — σ(11 or 12 layers) ;

Horizontal— Spectral representation T_{21}, T_{31}, T_{42}, T_{63}, T_{106},

Vertical—Finite difference representation ;

Transform method — Alias-free non-linear advection;

Time differencing — Semi-implicit, Asselin time filter $\gamma=0.5$ (Asselin 1972)

Horizontal diffusion — Linear (fourth order), following Kanamitsu *et al.* (1983)

$K = 2\times10^{15}$ m^4 s^{-1} (for ζ, T, S)

$K = 2\times10^{16}$ m^4 s^{-1} (for D)

Envelope-orography — $\bar{h}+2$ s.d. based on a basic data NAVY 10 minute resolution tape ;

Vertical boundary conditions — Kinematic, $\dot{\sigma}=0$ top and bottom ;

Data — ECMWF FGGE IIIb, NMC IIIa and ECMWF IIIa.

Initialization — Non-linear normal mode with physics, 5 vertical modes (Kitade 1983)

Physical processes

Large scale condensation — Disposition of supersaturation T, q ;

Dry convective adjustment — Kanamitsu (1975);

Shallow convection — Tiedtke and Slingo (1985);

Deep moist convection — Modified Kuo scheme, (Krishnamurti *et al.* 1983);

Planetary boundary layer — Surface fluxes are based on the similarity theory, vertical distribution of fluxes is Richardson number dependent;

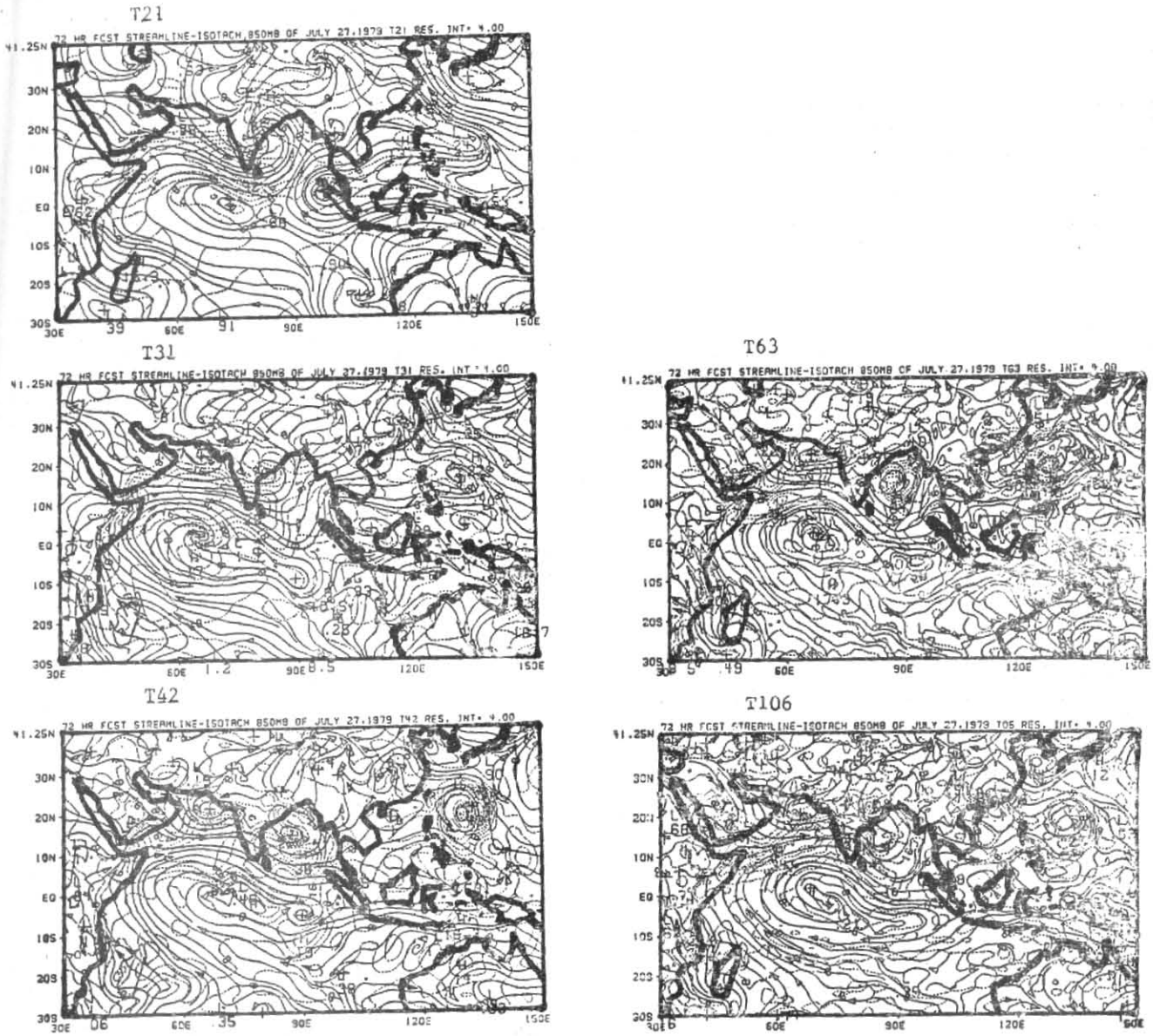

Fig. 1. 850 mb predicted streamline day 3

Radiative processes — Long wave radiation — Band model (Harshvardhan and Corsetti 1984) ;

Short wave radiation—Lacis and Hansen (1974). The model includes cloud feedback processes, threshold relative humidity to define clouds; diurnal change is introduced *via* a variable zenith angle ;

The surface temperature is based on 10-day mean SST values over the oceans ; the ground temperture is calculated from the surface energy balance over land and is coupled to surface fluxes and a surface hydrology is included (Krishnamurti *et al.* 1988a).

(B) *Horizontal resolution*

The triangular truncation of spherical harmonics appears somewhat better suited (as compared to the so called Rhomboidal Truncation) for tropical prediction within a global model. In the present study we have examined the results of integrations at 5 different horizontal resolutions : T_{21}, T_{31}, T_{42}, T_{63} and T_{106}. The number of transform grid points used for these truncations are : (64, 32), (96, 48), (128, 64), (192, 96) and (384, 160). Here the first number within the parenthesis denotes the number of transform points around a latitude circle while the second denotes the number of transform points (determined from the nodes of the associated Legendre functions) in the meridional direction from pole to pole.

(C) *Vertical discretization*

The vertical representations used in the present study have 12 layers ; its first computational level lies next to

the earth's surface ($\sigma = 1$) at $\sigma = \sqrt{0.99}$ which is roughly 5 mb from the earth's surface. A large sensitivity of the forecasts to the vertical resolution in the surface layer was found. Surface fluxes of heat, moisture and momentum are enhanced and contribute to tropical cyclogenesis. The vertical discretization of this model is based on Daley *et al.* (1976).

(D) *Orography*

The present study utilizes an envelope orography following Wallace *et al.* (1983) for the different resolutions of the global model. The basic data set for the representation of orography is derived from a U.S. Navy 10-minute high resolution terrain height tabulation. The mean value of the height $\bar{h}$ and the standard deviation are calculated for each Gaussian grid square for the respective resolutions over the globe. The model makes use of an envelope orography based on the relation: $h = \bar{h} + 2$ s.d.

(E) *Cumulus parameterization*

The present study is based on a modified Kuo's scheme as in Krishnamurti *et al.* (1983).

(F) *Planetary boundary layer*

This is another area of the physical parameterization to which the tropical cyclone predictions exhibit a large sensitivity. In this paper the surface layer fluxes of momentum, heat and moisture are calculated *via* the surface similarity theory following Businger *et al.* (1971) and Chang (1978). The vertical distribution of fluxes utilizes a Richardson number dependent mixing length concept. The large sensitivity is evident when one compares a poorly resolved with an explicitly resolved planetary boundary layer.

A detailed description of the surface similarity theory used in our models is presented in Krishnamurti and Bedi (1988b). The surface similarity fluxe estimates requires a knowledge of the wind, temperature and moisture across the constant flux layer. At the earth's surface ($\sigma = 1$) the following distinction is made between land and ocean : over land areas the ground temperature T_1 is obtained from the surface energy balance (over oceans the SST defines T_1), and the surface specific humidity q_1 is obtained as a function of the saturation specific humidity q_s, (at temperature T_1) and a ground wetness parameter. The wind at this level is set to zero, while the height of this surface is set to a roughness length z_0. The top of the constant flux layer is assumed to be at the next level, *i.e.*, $\sigma = \sqrt{.99}$ for the 12 layer (and $\sigma = \sqrt{.95}$ for the 11- layer model. At this level the model variables are. Temperature T and the dew point depression S. The wind at this level is obtained by an assumption of a log-linear wind law between the two lowest wind levels, $\sigma = 1$ and $\sigma = \sqrt{.99}$ (or $\sqrt{.95}$). The height z_2 at this level is obtained from a use of the hydrostatic law (with an appropriate virtual temperature correction between the levels $\sigma = 1$ and $\sigma = \sqrt{.99}$ (or $\sqrt{.95}$). The expressions for the stability dependent exchange coefficients contain in their denominator z_2/z_1 and $(z_2 - z_1)/z_1$ (*see, e.g.*, equations 24, 25, 26 and 27 in Krishnamurti *et al.* (1988b). Thus, a lowering of the thickness of the constant flux layer reduces z_2 and $z_2 - z_1$ with a marked increase the stability dependent exchange coefficients for heat, moisture and momentum. Overall we have noted that a lowering of the top of the constant flux layer from $\sigma = \sqrt{.95}$ to $\sigma = \sqrt{.99}$ increases the fluxes by almost a factor of two to three.

The first part of this paper addresses the formation of a monsoon depression during the period 27 July 1979 (1200 UTC) through 2 August 1979. Several medium range forecasts were carried out with the global model at the different resolutions starting from T_{21} through T_{106}. This was an active phase of the monsoon, the low level monsoon flow across the Indian subcontinent was quite strong. The depression formed over the northern Bay of Bengal on the 28 July and slowly moved westward.

The best forecasts of this storm were obtained at the resolution T_{106}. The position of the storm appeared to have a rather large influence on the placing of planetary scale divergent circulations. For instance, at the resolution the storm formed over southern India and the centre of the planetary scale divergent circulation was located over the region. The more correct placing was noted at the resolution T_{106} where the storm and the divergent outflow centre at 200 mb were both located over the northern Bay of Bengal.

As is to be expected, the precipitation amounts increase with resolution and were most realistic at the highest resolution.

Fig. 1 shows the 800 mb wind field on day 3, as predicted at the different coefficients. Also shown in this illustration is the analysis based on the observed wind. This illustration clearly shows the importance of increasing resolution. The predicted precipitation totals (mm) between hour 0 and hour 72 are shown in Fig. 2. Also shown in this illustration are those based on observations. It is apparent that the model, at the highest resolution, is better able to handle the rainfall than at the other resolutions. The shift of the divergent outflow centre at 200 mb as a function of resolution is illustrated in Fig. 3. Overall the forecasts in this example were quite reasonable to about 5 days at the highest resolution.

The following were some of the important factors in the current modelling effort for the medium range prediction of the monsoon :

(a) The use of envelope orography with the 2σ added to the mean height $\bar{h}$ improves the prediction of monsoon circulations over the Arabian Sea.

(b) The modified Kuo's scheme has a major impact on the monsoon forecasts.

(c) The delayed FGGE level IIIb data includes a rather detailed 4-D assimilation, that provided the best forecasts when they were compared to forecasts made with operational data sets.

(d) Explicitly resolving surface layer physics with computational levels across the constant flux layer improves monsoon forecasts immensely—in particular this has a positive impact on the monsoon precipitation fields.

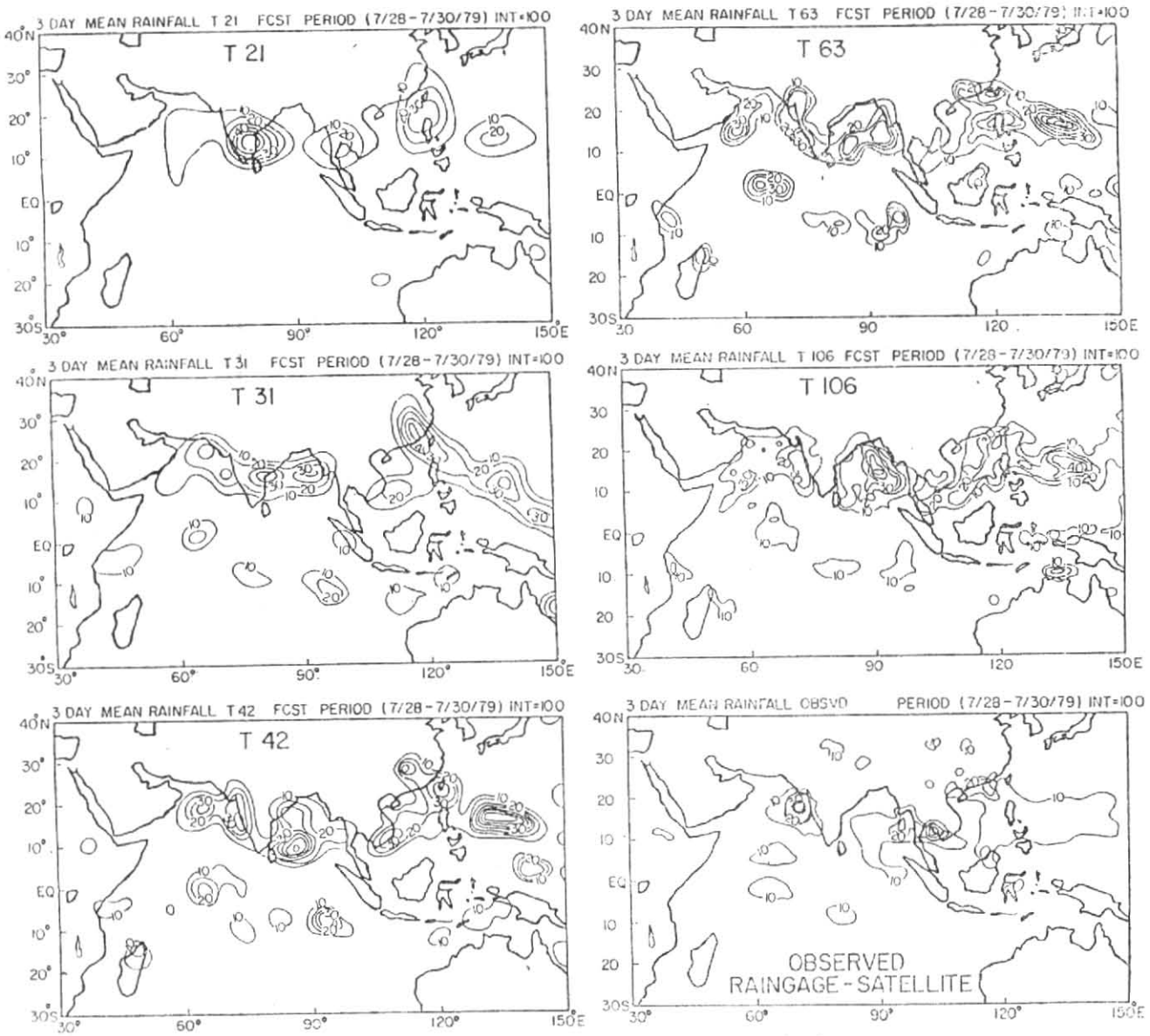

Fig. 2. Three-day mean precipitation day 0 to day 3

(e) The use of a sophisticated radiative, such as is used here, has a major impact on the strength of the monsoonal circulation.

(f) The increased horizontal resolution, as shown here, improves the circulations and winds.

2. Prediction of dry and wet spells on time scales of one month

Observations during the FGGE year and subsequent to that for the recent 8-year period have clearly shown the presence of low frequency motions on the time scale of roughly 30 to 50 days. There are several regional and global aspects of these oscillations that have been emphasized in recent literature. Among these we shall be addressing the following four observational aspects of low frequency motions :

(a) *Meridionally propagating 30 to 50 day waves in the lower troposphere of the monsoon region*—This is a family of trough-ridge systems that can be seen as the streamline-isotach charts of the time filtered motion field. The passage of a trough or a ridge line over central India generally coincides with the occurrence of a wet or a dry spell respectively. The meridional scale of this system is roughly 2000 to 3000 km. The speed of meridional motion is roughly 1° Lat./day. During certain years, the meridional motion and passage of these systems during the summer monsoon season is quite regular while over other years the motion is somewhat irregular. The reasons for this type of interannual behaviour are not quite clear at the present time.

(b) *Zonally propagating planetary scale divergent circulations on this time scale*—These seem to have a dominant scale of wave numbers 1 and 2. They traverse the globe, from west to east, in roughly 30 to 50 days. The largest amplitude is

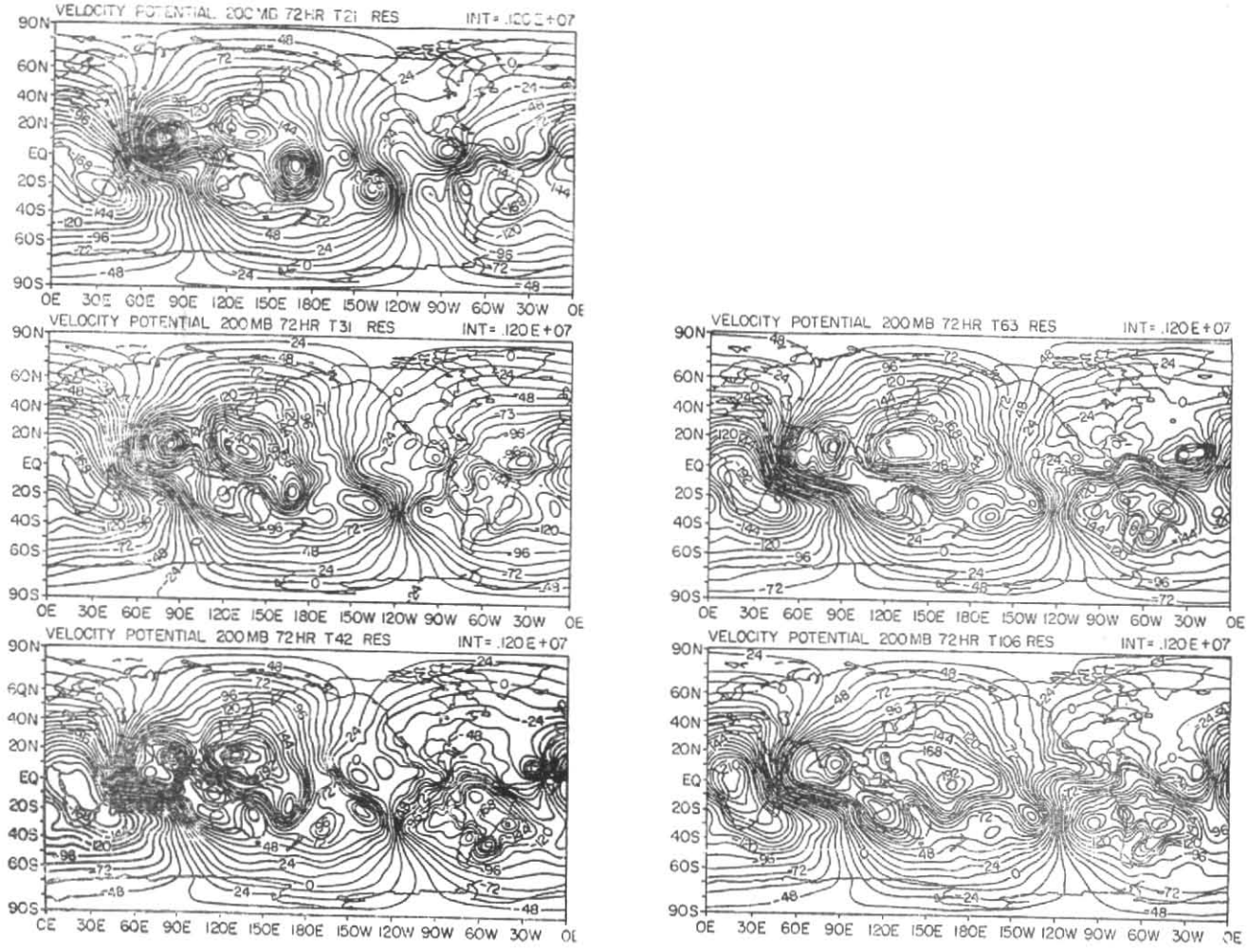

Fig. 3. 200 mb predicted velocity potential day 3

in the equatorial latitudes. The divergent circulations have a large meridional extent. the east-west circulations can be seen even as far as 35° N and 30° S. These broad divergent circulations appear to be related to equatorial and monsoonal heat sources and sinks. The interannual variation of these eastward propagating waves has also been studied and one finds that the propagations have been somewhat irregular during several recent years.

(c) An important aspect on this time scale is the air-sea interactions. We have recently examined the oceanic fluxes of sensible and latent heat on this time scale. When fluxes are calculated using the so-called 'surface similarity theory', the basic variables are the SST, the surface wind, the temperature and humidity at the top of a constant flux layer. The similarity fluxes are defined from expressions that invoke the Monin-Obukhov length and a non-linear coupling of the momentum, heat and moisture. Because of this non-linear coupling, one can diagnose the relative importance of the low frequency variations of SST, surface wind, air temperature and humidity and assess their role in the contribution to fluxes on this time scale. A detailed diagnostic study was recently completed by Krishnamurti *et al.* (1988). It was found that the latent heat flux on the time scale of 30 to 50 days can be as large as 10 to 20 watts/m², which was about 5 to 10% of the total flux over the Indian and Pacific Oceans. It was also noted that wind variations on this time scale were very important contributors; next in line were the contributions from SST variations on this time scale. The variations in air temperature and humidity were relatively less important. Although the amplitude of SST variation was only of the order of 0.8° to 1°C on the time scale, that coupled with wind variations of the order 3 to 5 ms^{-1} contributed to significant latent heat fluxes, *i.e.*, $\simeq$ 10 to 20 watts/m². The sign of these low frequency fluxes are preserved for a couple of weeks, thus their role can become significant.

(d) The maintenance of low frequency modes has been addressed *via* detailed computations of energetics in the frequency domain using daily globally analysed data sets over many years. These studies are somewhat analogous to the estimates on energetics in the zonal wave number domain. In the latter approach, one speaks of kinetic energy exchanges from zonal flows to eddies of certain scales, and of waves to waves *via* non-linear interactions. The other important interactions in the wave number domain are those from potential to kinetic energy for fixed zonal wave numbers. In the frequency domain, analogous selection rules govern the exchanges of energy. Here, one can visualize a breakdown among long term mean, low frequency and high frequency motions. In a frequency domain, the kinetic to kinetic energy exchanges can occur among long term time mean flows and other frequencies, or among triads of frequencies (analogous to the wave number domain). The potential to kinetic energy exchanges are restricted to occur at the same frequencies.

The results of these energetics calculations performed by Sheng (1986), show that the kinetic energy of low frequency modes on the time scale of 30 to 50 days are maintained by the following processes :

(*i*) They receive a substantial amount of kinetic energy from high frequency modes,

(*ii*) They loss kinetic energy to the long term time mean flow and

(*iii*) They receive a smaller amount of energy from the potential energy on the same frequencies.

The above observational findings were important for our design of experiments to increase the predictability of low frequency modes.

In this context, we should mention some results on the predictability of low frequency modes from long term integration of a global model. Dr. William Heckley, of the ECMWF, examined the presence (or absence) of the monsoonal low frequency modes from several ensembles of predicted data for the FGGE period. The zero day ensemble of 365 days is a string of the initialized FGGE data. This string, as to be expected, contained the meridionally propagating low frequency modes. However, as the strings of the ensemble of 1, 2, 3, 4 and 5-day forecasts were examined, in this context, it was noted that the low frequency modes were lost by about day 5. The conclusion was drawn that the global model has a predictability, for the low frequency modes, of about 4 days.

We feel strongly that this loss of predictability for the low frequency modes is largely due to the errors the model makes in the prediction of the higher frequency motions. These, in turn, contaminate the low frequency modes by the transfer of errors in these energy exchanges.

The aforementioned observations and ideas were useful in the design of a class of long term integration experiments in order to extend the predictability of low frequency modes.

Specifically, we designed the following experiments :

(a) A control experiment with a comprehensive global spectral model (Krishnamurti *et al.* 1989). The model was initialized using non-linear normal mode initialization using global data for 31 July 1979 (1200 UTC). This experiment included an annual cycle of SST. A 270-day integration was carried out starting from that day.

(b) A low frequency mode experiment where the initial state was obtained as follows :

(*i*) A time mean state was obtained for all variables at all vertical levels using the data sets for a 120-day period preceding the initial date (*i.e.*, 31 July 1979, 12 UTC),

(*ii*) A low frequency mode for the initial date, this was based on the data sets for the same preceding 120-day period,

(*iii*) SST anomalies on the time scale of 30 to 50 days. These were updated during the course of integration. This data is described by Krishnamurti *et al.* (1988). In order to enhance the response for the model resolution, the anomalies were multiplied by a factor of two,

(*iv*) A long term averaged annual cycle of SST that varies from month to month (The same fields were also used in the control experiment).

The premise here being that if the high frequency modes are filtered out from the initial state, the contamination for the energy transfers as errors grow could be reduced, thus we might extend the predictability of low frequency modes. The retention of the time mean state and the SST anomalies was to provide some of the other important energy sources for these low frequency modes.

The results of these experiments were quite successful to about 30 days, after which the energy exchanges grew quite large as high frequency motions evolved. The main results of these experiments were as follows :

(a) The control experiment failed to predict meridional motion of low frequency modes. The anomaly experiment was quite successful. The meridionally propagating low frequency modes of the lower troposphere over the Asian monsoon region were very accurately predicted for the first 30 days. The occurrence of a dry spell over central India in the middle of August was well predicted. The amplitude of the low frequency mode was somewhat underpredicted, however, the phase errors were very small.

(b) The eastward propagating planetary scale divergent wave at 200 mb was very reasonably predicted to almost 25 days in the anomaly experiment. The phase speed was very close to that based on observations. The control experiment failed to show an eastward motion of the divergent wave.

(c) The energetics of the control revealed a large transfer of kinetic energy from the low frequency modes to the higher frequencies. That must be an important factor for the rapid collapse of predictability in the control experiment. In the anomaly experiment (where we had included a time mean state, a low frequency mode and the SST anomalies on the time scale of 30-50 days), the kinetic energy exchange was consistent with the observational results. This experiment was extended to 270 days. The energetics in the frequency domain were calculated for the 270 days of data and also from day 31 to day 270. As stated earlier, the predictability of the low frequency modes was good to about 30 days in this experiment. For the entire 270-day period, the kinetic energy exchange from the high to the low frequencies was positive, but greater than that for the period day 31 to day 270. This implies that the contributions from the first 30 days, for which the predictability was large, was consistent with the observational estimates. As the errors grow, the contribution to the energy exchange slowly reversed signs and the low frequency modes were contaminated.

3. Conclusion

The present approach simply delays the rate of contamination of low frequency modes, thus extending their predictability to almost one month. Eventually, higher frequency motions do form and the rate of contamination increases rapidly.

Further work is needed to assess the relative importance of the details of the time mean, the definition of the low frequency mode and the details of the SST anomalies in the increase of predictability of low frequency modes. Further experimentation is needed to predict the irregular behaviour of low frequency modes, as was noted from the observations from some recent years. If such experimentation is successful in predicting the irregular behaviour, then there is a need to diagnose the importance of the aforementioned input parameters.

This approach may hold much promise for predicting the dry and wet spells that are related to the passage of low frequency modes on the intraseasonal time scales.

Acknowledgements

This research was supported by the National Science Foundation, NSF grant No. ATM 83-04809 and the National Oceanic and Atmospheric Administration (NOAA) grant No. NA 87AA-D-AC038.

References

Asselin, R., 1972, Frequency filter for time integrations, *Mon. Weath. Rev.*, **100**, 487-490.

Businger, J.A., Wyngaard, J.C., Izumi, Y. and Bradley, E.F., 1971, Flux profile relationship in the atmospheric surface layer, *J. atmos. Sci.*, **28**, 181-189.

Chang, L.W., 1978, Determination of surface flux of sensible heat, latent heat and momentum utilizing the Bulk Richardson number, *Papers in Met. Res.*, **1**, 16-24.

Daley, R.C., Girard, C., Henderson, J. and Simmonds, I., 1976, Short-term forecasting with a multi-level spectral primitive equation model : Part 1—Model formulation, *Atmosphere*, **14**, 98-116.

Harshvardhan and Corsetti, T.G., 1984, Longwave parameterization for the UCLA/GLAS GCM, NASA Tech. Mem. 86072, Goddard Space Flight Centre, Greenbelt, MD.

Kanamitsu, M., Tada, K., Kudo, K., Sato, N. and Isa, S., 1983, Description of the JMA operational spectral model, *J. met. Soc. Japan*, **61**, 812-828.

Kanamitsu, M., 1975, On numerical prediction over a global tropical belt, Report No. 75-1, Dept. of Meteorology, Florida State University, Tallahassee, Florida, 32306, pp. 1-282.

Kitade, T., 1983, Nonlinear normal mode initialization with physics, *Mon. Weath. Rev.*, **111**, 2194-2213.

Krishnamurti, T.N., Low-Nam, S. and Pasch, R., 1983(a), Cumulus parameterization and rainfall rates : II, *Mon. Weath. Rev.*, **111**, 815-828.

Krishnamurti, T.N., Pasch, R.J. Pan, H.L., Chu, S. and Ingles, K., 1983(b), Details of low latitude medium range numerical weather prediction using a global spectral model I, *J. met. Soc. Japan*, **61**, 188-207.

Krishnamurti, T.N., Bedi, H.S., Heckley, W. and Ingles, K.J., 1988(a), On the Reduction of Spin-Up Time for Evaporation and Precipitation in a Global Spectral Model, *Mon. Weath. Rev.*, **116**, 4, pp. 907-920.

Krishnamurti, T.N. and Bedi, H.S., 1988(b), Cumulus parameterization and rainfall rates : III, *Mon. Weath. Rev.*, **116**, 3, pp. 583-599.

Krishnamurti, T.N., Oosterhof, D. and Mehta, A., 1988, Air-sea interaction on the time scale of 30 to 50 days during FGGE, *J. atmos. Sci.*, **45**, 1304-1322.

Lacis, A.A. and Hansen, J.E., 1974, A parameterization for the absorption of solar radiation in the earth's atmosphere, *J. atmos. Sci.*, **31**, 118-133.

Sheng, Jian, 1986, On the energetics of low frequency motions, Report No. 86-14, Dept. of Met., Florida State Univ., Tallahassee, Florida, 32306, pp. 1-171.

Tiedtke, M. and Slingo, J., 1985, Development of the operational parameterization scheme, ECMWF Research Dept. Tech. Memo. No. 108, 38 pp.

Wallace, J.M., Tibaldi, S. and Simmons, A.J., 1983, Reduction of systematic forecast errors in the ECMWF model through the introduction of envelope orography, *Quart. J. R. met. Soc.*, **109**, 683-718.